A MULTIMODE INTERFERENCE COUPLER WITH EXPONENTIALLY TAPERED WAVEGUIDE

J.-J. Wu

Department of Physics
Shandong University of Technology
No. 12 ZhangZhou Road, Zibo, Shandong Province, P. R. China

Abstract—An exponentially tapered structure is introduced into multimode interference (MMI) devices. Compared with a parabolically tapered structure, which has been successfully used in MMI devices, this structure can further reduce the length of these devices. The performances of the 1×2 MMI coupler with exponentially tapered structure, such as the optical transmission, the wavelength response and the fabrication tolerance, are investigated by the 2D finite difference beam propagation method. Results show that the exponentially tapered MMI coupler exhibits a similar property to that with a parabolically tapered structure.

1. INTRODUCTION

As an important element in integrated optics, 1×2 couplers are widely used as optical splitter and optical combiner. In recent years, multimode interference (MMI) couplers based on self-imaging effects have attracted more and more popularity in the design of integrated optical circuits due to its advantages such as compactness, better manufacturing tolerances, insensitivity to polarization, and large bandwidth [1]. The MMI technology main drawback is that couplers tend to be large if we are trying to obtain low loss and high accuracy. In order to reduce the MMI device size, a new kind of MMI structure with a parabolically tapered width has been proposed [2, 3]. Such tapered MMI couplers based on InP-InGaAsP and silicon-on-insulator (SOI) waveguides have been realized [4–7]. Compared with the conventional MMI structures, the parabolically tapered structure can reduce the length of the MMI devices. The benefits and drawbacks of the use of the parabolically tapered in MMI devices, in comparison with the straight MMI devices, have also been

investigated [8–10]. In [11], we propose another exponentially tapered structure for the same purpose. The use of exponential tapers for the design of more ultracompact 4×4 MMI photonic switch has been reported [12]. But such kind of tapered waveguide is just a special example of our proposed exponentially tapered structure. Compared with the parabolically tapered, which has been successfully used in the MMI devices, this structure can further reduce the length of the MMI devices. In this article, a detailed analysis of the performance of this kind of MMI devices is presented. It is shown that the performance of the MMI couplers with the exponentially tapered structure is similar to the devices with the parabolically tapered structure.

Many numerical approaches have been developed to analyze general dielectric waveguides in different aspects [13–26]. Compared with other numerical techniques, the beam propagation method (BPM) which automatically includes the effects of both guided and radiating fields as well as mode coupling and conversion, is the most popular and powerful numerical technique for modeling guided-wave photonic devices and most commercial software for such modeling is based on it [26]. To date numerous algorithms for BPM have been proposed and successfully applied to a very wide class of dielectric optical waveguide structures. In this paper, the 2D finite difference beam propagation method (FD-BPM) is used in the simulation.

2. THEORY

The 1×2 MMI coupler is composed of a single-mode input waveguide, a multimode waveguide, and two single-mode output waveguides. The structure of the compact tapered 3-dB MMI coupler is illustrated in Figure 1. In Figure 1, d is the offset for output waveguides from the
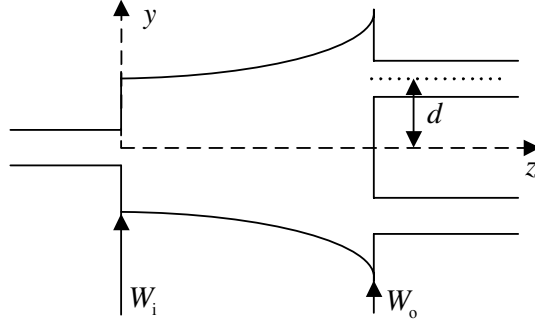

Figure 1. Schematic diagram of a 1×2 tapered MMI coupler.

center of the multimode waveguide. The multimode waveguide width is exponentially tapered according to

$$W(z) = W_{\mathrm{i}} + A \left[\exp\left(\frac{gz}{L_{\mathrm{MMI}}} \right) - 1 \right] \tag{1}$$

$$A = (W_{\mathrm{o}} - W_{\mathrm{i}})/(\exp(g) - 1) \tag{2}$$

where z is the direction of propagation of the light, L_{MMI} is the length of the tapered MMI section, W_{i} is the width of the MMI section at $z = 0$ and W_{o} is that at $z = L_{\mathrm{MMI}}$, and g is a parameter associated with the shape of the profile. The input waveguide is located at the center of the start wall of the tapered MMI section, and the two output waveguides are located at $W_{\mathrm{o}}/4$ and $3W_{\mathrm{o}}/4$, respectively, on the end wall of the tapered MMI section. For Eq. (1), if g is $\ln(W_{\mathrm{o}}/W_{\mathrm{i}})$, then the tapered structure here mentioned become the exponential structure which has been used [12].

Assuming the multimode waveguide supports m lateral modes with mode numbers $v = 0, 1, 2, \ldots, (m-1)$ at a free space wavelength λ, the effective index of the multimode waveguide section and the lateral confinement section is n_{r} and n_{c}. According to the dispersion equation, the lateral wave number, k_{vy}, and the propagation constant β_v are related as follows

$$k_{vy}^2 + \beta_v^2 = k_0^2 n_{\mathrm{r}}^2 \tag{3}$$

where, $k_0 = 2\pi/\lambda$, $k_{vy} = (v+1)\pi/W_{\mathrm{e}}(z)$, and $W_{\mathrm{e}}(z)$ is the effective width of the MMI section

$$W_{\mathrm{e}}(z) = W(z) + W_g \tag{4}$$

The Gooss-Hänchen shift W_g is determined by

$$W_g = \left(\frac{\lambda}{\pi} \right) \left(\frac{n_{\mathrm{c}}}{n_{\mathrm{r}}} \right)^{2\sigma} \left(n_{\mathrm{r}}^2 - n_{\mathrm{c}}^2 \right)^{-1/2} \tag{5}$$

where $\sigma = 0$ for transverse electric (TE) mode and $\sigma = 1$ for transverse magnetic (TM) mode.

The propagation constants β_v can be deduced from Eq. (3)

$$\beta_v \approx k_0 n_{\mathrm{r}} - \frac{(v+1)^2 \pi \lambda}{4 n_{\mathrm{r}} W_{\mathrm{e}}^2(z)} \tag{6}$$

Therefore, the phase change between the v order mode and the fundamental mode over the exponentially tapered waveguide can be

given by

$$\Delta\phi = (\beta_0 - \beta_v)\, L_{\text{MMI}} = \int_0^{L_{\text{MMI}}} (\beta_0 - \beta_v)dz$$

$$= v\,(v+2)\,\frac{\pi\lambda}{4n_{\mathrm{r}}} \int_0^{L_{\text{MMI}}} \frac{dz}{W_{\mathrm{e}}^2\,(z)} \qquad (7)$$

Substitute Eqs. (1), (2), (4) and (5) into Eq. (6) yields

$$\beta_0 - \beta_v = \frac{v\,(v+2)\,\pi\lambda\gamma}{4n_{\mathrm{r}}W_{\mathrm{o}}^2} \qquad (8)$$

where

$$\gamma = \frac{W_{\mathrm{o}}^2}{(W_g + W_{\mathrm{i}} - A)^2} - \frac{W_{\mathrm{o}}^2}{g\,(W_g + W_{\mathrm{i}} - A)^2}\ln\left(\frac{W_g + W_{\mathrm{o}}}{W_g + W_{\mathrm{i}}}\right)$$
$$- \frac{W_{\mathrm{o}}^2\,(W_{\mathrm{o}} - W_{\mathrm{i}})}{g\,(W_g + W_{\mathrm{i}} - A)\,(W_g + W_{\mathrm{o}})\,(W_g + W_{\mathrm{i}})} \qquad (9)$$

The beat length, L_{π}^e, of the two lowest-order modes is

$$L_{\pi}^e = \frac{\pi}{\beta_0 - \beta_1} = \frac{4n_{\mathrm{r}}W_{\mathrm{o}}^2}{3\gamma\lambda} \qquad (10)$$

For the parabolically tapered structure, the beat length of the two lowest-order modes can similarly obtained

$$L_{\pi}^p = \frac{\pi}{\beta_0 - \beta_1} = \frac{4n_{\mathrm{r}}W_{\mathrm{o}}^2}{3\alpha\lambda} \qquad (11)$$

where

$$\alpha = \frac{W_{\mathrm{o}}^2}{2\,(W_g + W_{\mathrm{i}})\,(W_g + W_{\mathrm{o}})} + \frac{W_{\mathrm{o}}^2\,\tan^{-1}\,[(W_{\mathrm{o}} - W_{\mathrm{i}})/(W_g + W_{\mathrm{i}})]^{1/2}}{2\,(W_{\mathrm{o}} - W_{\mathrm{i}})^{1/2}\,(W_g + W_{\mathrm{i}})^{3/2}} \qquad (12)$$

For the structure shown in Figure 1, the input single-mode waveguide is located at the center of the start wall of tapered MMI section, and only even-symmetric modes are excited in the tapered MMI section. Then two symmetric interference images can be formed, with a length of

$$L_{\text{MMI}}^i = (3/8)\, L_{\pi} \qquad (13)$$

where i is e and p for the exponentially tapered structure and the parabolically tapered structure respectively.

Comparing (10) and (11), we can see the difference of the beat length of the two lowest-order modes between the parabolically and the exponentially tapered structure. The beat length has relationship with the parameters γ and α. Obviously, the larger the value of γ (or α) is, the shorter the length of the MMI section is. Figure 2 illustrates profiles of γ and α as a functions of the normalized width variation $d\Omega$, $d\Omega = (W_o - W_i)/W_o$, for TE mode. In our calculation, a value of $n_r = 1.47$ and $n_c = 1.40$ is chosen, the width of the tapered MMI section at $z = L_{\mathrm{MMI}}$, W_o, is $24\,\mu\mathrm{m}$, and g is 5. It can be seen from Figure 2, γ is larger than α. Then for the MMI couplers with same width at the start wall and the end wall of the tapered MMI section, the length of MMI section with exponential taper is shorter than the length of that with parabolic taper. It is very favorable for realizing of ultracompact MMI devices. So this exponentially tapered structure will be a good candidate compared with the parabolically tapered structure, which has been successfully used in many MMI devices.
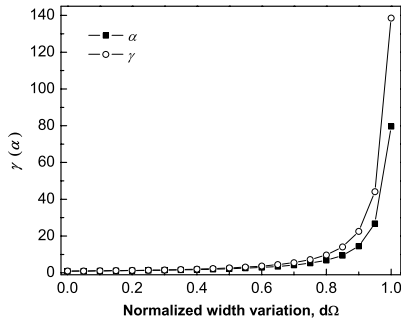

Figure 2. γ and α versus the normalized width variation.
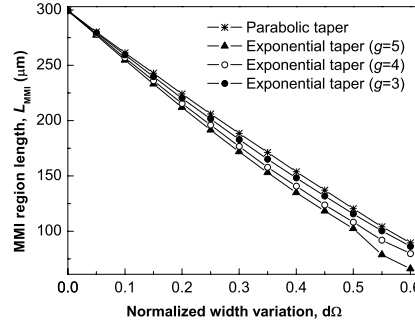

Figure 3. Variation of the MMI length for a tapered MMI coupler with the normalized width.

3. NUMERICAL SIMULATION AND RESULTS

In order to demonstrate the performance of the exponentially tapered structure, a 1×2 MMI coupler is simulated with a 2D beam propagation method (BPM) based on the finite-difference method. The simulations utilized the Padé $(2, 2)$ approximation in order to minimize phase errors in the propagation equation at wide angles. In addition, in order to prevent spurious reflection from the computational window edges, the transparent boundary (TBC) is used. In our calculation, the free space wavelength is $1.55\,\mu\mathrm{m}$ and only TE modes are considered. The other parameters are same as those used in Figure 2.
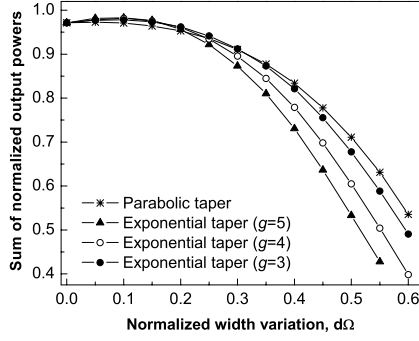
Figure 4. Sum of normalized powers in output waveguides with normalized width variation.
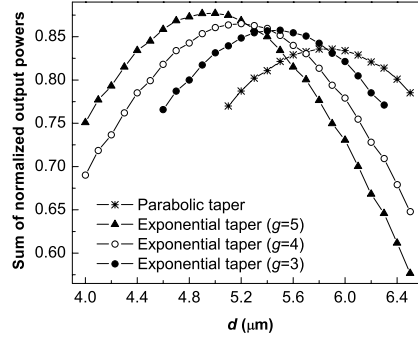
Figure 5. Sum of normalized powers in output waveguides versus offset d.

The Variation of the MMI length for a 3-dB tapered MMI coupler with the normalized width is shown in Figure 3. For each $d\Omega$, the imaging length, L_{MMI}, is obtained via a series of simulations in which L_{MMI} is allowed to vary in order to maximize the total power, defined as the sum of the powers in each of the output ports. The sum of the powers at this particular imaging length of the device at each value of $d\Omega$ is also presented in Figure 4. As can be see from the Figure 3, the parabolically tapered structure gives the longest devices, as expected, for all the normalized width variation values except at $d\Omega = 0$, and the exponentially tapered structure with $g = 5$ yield the shortest devices length. For all the tapered MMI devices, the imaging length L_{MMI} varies approximately linearly with $d\Omega$ as show in Figure 3. The properties of optical transmission of the MMI devices with different tapered structure as a function of the normalized width variation are similar (see Figure 4). The transmission losses increase with $d\Omega$. But the loss rate is different for these devices. Though the exponentially tapered structure with $g = 5$ has the lowest imaging length, it has the largest transmission loss when the $d\Omega$ exceeds 0.2.

In above simulation, the location of the output waveguides keeps at $W_{\mathrm{o}}/4$ and $3W_{\mathrm{o}}/4$, i.e., offset $d = 6\,\mu\mathrm{m}$. The location of the output imaging obtained from the self-imaging theory usually has a shift compared with practical imaging location. As MMI devices are sensitive to the phase changes, the tapered structure makes this shift more serious. In Figure 5, the sum of the powers in the output waveguides as a function offset d at $d\Omega = 0.4$ is given. The simulation results show that the tapered structure has an influence on the imaging location. For each kind of tapered MMI devices, we can see from Figure 5, there is an optimum value, at which the MMI devices have

the smallest transmission loss. We can also see from Figure 5, for each optimum output waveguide location, the sum of output powers of the exponentially tapered MMI devices is larger than the sum of that of the parabolically tapered MMI device.

Furthermore, the wavelength response characteristics of the tapered MMI devices at $d\Omega = 0.4$ are also obtained and shown in Figure 6. In our calculation, the optimum output waveguide location and the practical imaging length are used. The results show that the MMI devices with the exponentially tapered structure and the parabolically tapered structure have the same wavelength response characteristics.

Next, the width tolerances for the tapered MMI devices are also investigated and the sum of output powers with the width variation ΔW is shown in Figure 7. In our calculation, both the initial with W_i and the end width W_o of MMI section vary simultaneously. The results show that all of the examined devices exhibit same width tolerances sensitivity to the width variation. It can also be noticed that all the examined devices are fond to be less sensitivity to the positive width variation. So, during the devices fabrication, enlarging the width of the tapered MMI devices can't have large influence on the performance of the tapered MMI devices.
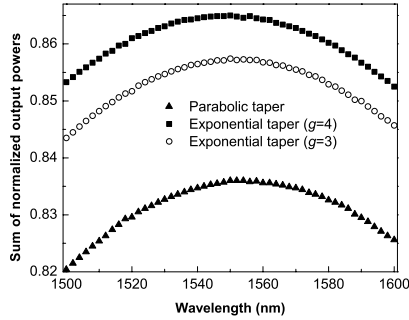

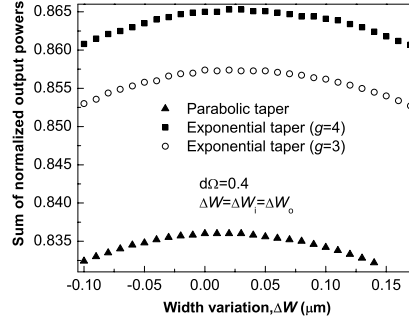**Figure 6.** Wavelength response for tapered MMI devices.

Figure 7. Fabrication tolerance for tapered MMI devices.

4. CONCLUSION

In order to reduce the scale, an exponentially tapered multimode waveguide is proposed to be used in the MMI devices. The relation between the length of the multimode waveguide and the parameters of the tapered structure is analyzed in theory. Compared with the parabolically tapered structure, which has been successfully used in

the MMI devices, this structure can further reduce the length of the MMI devices. The results of the simulation given by the wide-angle finite difference beam propagation method (FD-BPM) show that the performance of the MMI couplers with the exponentially tapered structure is similar to the devices with the parabolically tapered structure. As a result, the exponentially tapered structure will be a good candidate compared with the parabolically tapered structure.

REFERENCES

1. Soldano, L. B. and E. C. M. Pennings, "Optical multimode interference devices based on self-imaging: Principles and applications," *J. Lightw. Technol.*, Vol. 13, No. 4, 615–627, 1995.

2. Levy, D. S., R. Scarmozzino, Y. M. Li, and R. M. Osgood, Jr., "A new design for ultracompact multimode interference-based 2×2 couplers," *IEEE Photon. Technol. Lett.*, Vol. 10, No. 1, 96–98, 1998.

3. Levy, D. S., R. Scarmozzino, and R. M. Osgood, Jr., "Length reduction of tapered $N \times N$ MMI devices," *IEEE Photon. Technol. Lett.*, Vol. 10, No. 6, 830–832, 1998.

4. Levy, D. S., K. H. Park, R. Scarmozzino, R. M. Osgood, Jr., C. Dries, P. Studerkov, and S. Forrest, "Fabrication of ultracompact 3-dB 2×2 MMI power splitters," *IEEE Photon. Technol. Lett.*, Vol. 11, No. 8, 1009–1011, 1999.

5. Wei, H. Z., J. Z. Yu, Z. L. Liu, X. F. Zhang, W. Shi, and C. S. Fang, "Fabrication of 2×2 tapered multimode interference coupler," *Electron. Lett.*, Vol. 36, No. 19, 1618–1619, 2000.

6. Wei, H. Z., J. Z. Yu, Z. L. Liu, X. F. Zhang, W. Shi, and C. S. Fang, "Fabrication of 4×4 tapered MMI coupler with large cross section," *IEEE Photon. Technol. Lett.*, Vol. 13, No. 5, 466–468, 2001.

7. Wei, H. Z., J. Z. Yu, X. F. Zhang, and Z. L. Liu, "Compact 3-dB tapered multimode interference coupler in silicon-on-insulator," *Opt. Lett.*, Vol. 26, No. 12, 878–880, 2001.

8. Wei, H. Z., J. Z. Yu, Z. L. Liu, X. F. Zhang, W. Shi, and C. S. Fang, "Signal bandwidth of general $N \times N$ multimode interference couplers," *J. Lightw. Technol.*, Vol. 19, No. 5, 739–745, 2001.

9. Yan, Q. F., J. Z. Yu, and Z. L. Liu, "Size tolerance analysis of a 4×4 tapered multimode interference," *Opt. Eng.*, Vol. 42, No. 8, 2235–2239, 2003.

10. Themistos, C., M. Rajarajan, B. M. A. Rahman, S. S. A. Obayya, and K. T. V. Grattan, "Rigorous comparison of parabolically tapered and conventional multimode-interference-based 3-dB power splitters in InGaAsP/InP waveguides," *Appl. Opt.*, Vol. 43, No. 27, 5228–5235, 2004.

11. Wu, J. J., B. R. Shi, and M. Kong, "Exponentially tapered multimode interference couplers," *Chin. Opt. Lett.*, Vol. 4, No. 3, 167–169, 2006.

12. Chang, W. C., C. H. Lien, P. J. Tsai, and H. J. Wang, "An ultracompact 4×4 photonic switch based on tapered multimode interference," *The 11th IEEE International Symposium on Electron Devices for Microwave and Optoelectronic Applications (EDMO 2003)*, 267–272, Orlando, Florida, USA, November 2003.

13. Watanabe, K. and K. Kuto, "Numerical analysis of optical waveguides based on periodic fourier transform," *Progress In Electromagnetics Research*, PIER 64, 1–21, 2006.

14. Faryad, M. and Q. A. Naqvi, "Fractional rectangular waveguide," *Progress In Electromagnetics Research*, PIER 75, 383–396, 2007.

15. Chang, H.-W. and M.-H. Sheng, "Field analysis of dielectric waveguide devices based on coupled transverse-mode integral equation — Mathematical and numerical formulations," *Progress In Electromagnetics Research*, PIER 78, 329–347, 2008.

16. Zhou, X. and G. W. Pan, "Application of physical spline finite element method (PSFEM) to fullwave analysis of waveguides," *Progress In Electromagnetics Research*, PIER 60, 19–41, 2006.

17. Talebi, N. and M. Shahabadi, "Application of generalized multipole technique to the analysis of discontinuities in substrate integrated waveguides," *Progress In Electromagnetics Research*, PIER 69, 227–235, 2007.

18. Talebi, N. and M. Shahabadi, "Analysis of a lossy microring using the generalized multipole technique," *Progress In Electromagnetics Research*, PIER 66, 287–299, 2006.

19. Dwari, S., A. Chakrabarty, and S. Sanyal, "Analysis of linear tapered waveguide by two approaches," *Progress In Electromagnetics Research*, PIER 64, 219–238, 2006.

20. Rostami, A. and H. Motavali, "Asymptotic iteration method: a powerful approach for analysis of inhomogeneous dielectric slab waveguides," *Progress In Electromagnetics Research B*, Vol. 4, 171–182, 2008.

21. Hernandez-Lopez, M. A. and M. Quintillan-Gonzalez, "A finite element method code to analyse waveguide dispersion," *Journal of Electromagnetic Waves and Applications*, Vol. 21, No. 3, 397–408, 2007.

22. Ooi, B. L. and G. Zhao, "Element-free method for the analysis of partially-filled dielectric waveguides," *Journal of Electromagnetic Waves and Applications*, Vol. 21, No. 2, 189–198, 2007.

23. Park, J. K., J. N. Lee, D. H. Shin, and H. J. Eom, "Full wave analysis of a coaxial waveguide slot bridge using the Fourier transform technique," *Journal of Electromagnetic Waves and Applications*, Vol. 20, No. 2, 143–158, 2006.

24. El Sabbagh, M. A. and M. H. Bakr, "Analytical dielectric constant sensitivity of ridge waveguides filters," *Journal of Electromagnetic Waves and Applications*, Vol. 20, No. 3, 363–374, 2006.

25. Khalaj-Amirhosseini, M., "Analysis of longitudinally inhomogeneous waveguides using Taylors series expansion," *Journal of Electromagnetic Waves and Applications*, Vol. 20, No. 8, 1093–1100, 2006.

26. Scarmozzino, R., A. Gopinath, R. Pregla, and S. Helfert, "Numerical techniques for modeling guided wave photonic devices," *IEEE J. of Selected Topics in Quantum Electron.*, Vol. 6, No. 1, 150–162, 2000.